Available online at www.sciencedirect.com
SCIENCE DIRECT
Bioorganic & Medicinal Chemistry 14 (2006) 2935–2941
Bioorganic & Medicinal Chemistry

# Novel fluorescent markers for hypoxic cells of naphthalimides with two heterocyclic side chains for bioreductive binding

Yan Liu,[a,b] Yufang Xu,[a,b,*] Xuhong Qian,[a,b,*] Jianwen Liu,[a] Liyun Shen,[a] Junhui Li[c] and Yuanxing Zhang[c]

[a]*School of Pharmacy, East China University of Science and Technology, Shanghai 200237, China*
[b]*Shanghai Key Laboratory of Chemical Biology, Shanghai 200237, China*
[c]*State Key Laboratory of Bioreactor Engineering, East China University of Science and Technology, Shanghai 200237, China*

Received 9 November 2005; revised 2 December 2005; accepted 3 December 2005
Available online 5 January 2006

**Abstract**—Novel naphthalimides with two heterocyclic side chains of 2-nitroimidazole for bioreductive binding were designed, synthesized, and used as fluorescent markers for hypoxic cells. Their evaluation for imaging tumor hypoxia was carried out in V79 cells, CHO cells, and 95D cells in vitro by using fluorescence scan ascent. $\mathbf{A_2}$ and $\mathbf{A_4}$ showed a very large differential fluorescence between hypoxic and oxic cells (V79 cells) in vitro and are promising candidate markers for hypoxic cells.


## 1. Introduction

Hypoxic (poorly oxygenated) cells in some human solid tumors are thought to limit the effectiveness of radiotherapy and chemotherapy, and in some cases may contribute to failure to control the disease, as most of solid tumor cells are hypoxic. Therefore, both before and during therapy, measurement of the hypoxic cell fraction in tumors could be of considerable clinical significance. On the basis of the oxygen status of their tumors, optimal treatment schedule could be devised for individual patients.[1]

In the past, various methods have been proposed for determining the hypoxic cell fraction in tumors, such as oxygen electrodes, histomorphometric analysis, DNA strand breaks, etc.,[2] but most of these direct techniques have been restricted for their invasion. A simpler and easier especially non-invasive method for identifying hypoxic cells is suggested to be the use of fluorescent nitroaromatic compounds. The nitro group quenches the fluorescence of the aromatic ring system, but on bioreduction of the nitro group in hypoxic cells the compound becomes more fluorescent.[3] The oxygen-dependent bioreductive metabolism of 2-nitroimidazoles proceeds in cells as a series of one-electron reductions. However, the nitro-radical anion, produced by the first one-electron reduction step, is very reactive toward oxygen and is oxidized back to the parent nitroimidazole.[4] Under hypoxic conditions, bioreductive metabolism leads to further stepwise reduction of the one-electron reduction product to the nitroso ($2e^-$) hydroxylamine ($4e^-$) and amine ($6e^-$) derivatives. Eventually, fragmentation of the imidazole ring occurs with reactive portions of the molecule binding to macromolecular components of cells in tissues and tumors.[5–7] The cellular metabolites of nitroaromatic compounds such as nitronaphthalimides in hypoxic cells were detected by the HPLC analysis, which was found to be amine.[3,8] Numerous nitroaromatic structures have been evaluated in model experiments in vitro. Although some interesting results have been obtained, the high affinity of the compounds to DNA could make the probe become localized to blood vessels or the nuclear region of well-oxygenated cells in tumors and fail to reach those hypoxic cells, which would decrease the efficiency of the hypoxic markers in vivo.[9]

Naphthalimides with single side chain of 2-nitroimidazole have been reported (Fig. 1) as hypoxic cell markers

*Keywords*: Fluorescent markers; Hypoxic cells; Naphthalimides; Bioreductive binding; 2-Nitroimidazole.
* Corresponding authors. Tel.: +86 0 21 64253589; fax: +86 0 21 64252603; e-mail addresses: yfxu@ecust.edu.cn; xhqian@ecust.edu.cn

0968-0896/$ - see front matter © 2005 Elsevier Ltd. All rights reserved.
doi:10.1016/j.bmc.2005.12.012

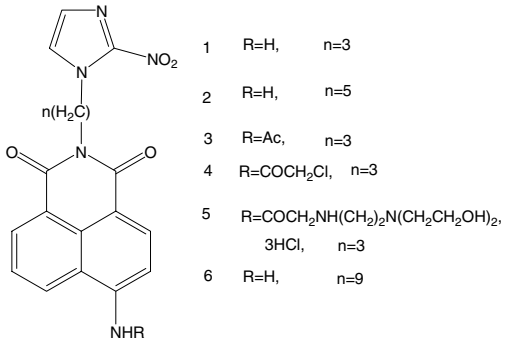


**Figure 1.** Reported naphthalimide fluorescent markers for hypoxic cells.

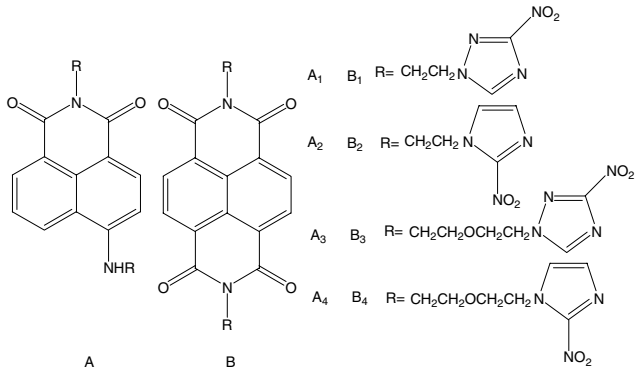


**Figure 2.** Novel fluorescent markers for hypoxic cell.

by using flow cytometry and a promising hypoxic–oxic differential could be reached. It was reported that in the experiments in vivo, the increase of the length of the side imide chain for compounds (**1**, **2**, and **6**) had little effect on the cell-uptake. However, the cell uptake of compound **5** was lower than those of other compounds. It was possible that the long side chain of **5** on the 4-position of the naphthalimide ring may interfere with its intercalation to DNA.[10] It means that the side chain has a very important effect on the property of fluorescent marker by comparing with the role of naphthalimide fluorophore. Therefore, in this paper, we will study a series of novel naphthalimides containing two heterocyclic side chains of 2-nitroimidazole and use convenient fluorescence microscopy and fluorescence scan ascent to collect fluorescence in cells, as flow cytometry was complicated for use and not easily available to common researchers.

We designed, synthesized and evaluated fluorescent markers containing two heterocyclic side chains with 2-nitroimidazole for several considerations: (1) The increased bioreductive parts (two 2-nitroimidazole moieties) could fix the fluorescent reduction products within the hypoxic cells stronger than one; (2) The length of linkers between 2-nitroimidazole and naphthalimide was modulated in this series of compounds, a longer linker also could avoid the possibility of fluorescence quenching by energy or electron transfer between the naphthalimide nucleus and the reduction states of the electron-deficient nitroimidazole moiety; (3) The two and longer linker would decrease markers' DNA intercalation or affinity, as only naphthalimides and their aromatic heterocycles without or with small substitutents show strong DNA intercalation or affinity; (4) In the fluorescent hypoxic probes described here, hydrophilic group (ether moiety) was introduced into the side chains of $\mathbf{A_3}$ and $\mathbf{A_4}$, $\mathbf{B_3}$ and $\mathbf{B_4}$ to promote its water solubility, thus transport in vivo to tumor cells was expected to be improved. Therefore, two novel fluorescent markers for hypoxic cells $\mathbf{A_2}$ and $\mathbf{A_4}$, $\mathbf{B_2}$ and $\mathbf{B_4}$ were designed (Fig. 2). Meanwhile, 3-nitro-l, 2, 4-triazole was also used as an alternative of 2-nitroimidazole (compounds $\mathbf{A_1}$ and $\mathbf{A_3}$, $\mathbf{B_1}$ and $\mathbf{B_3}$), however very weak fluorescence efficiencies were obtained when incubated with hypoxic cells.

## 2. Results and discussion

### 2.1. Syntheses and spectra

Compounds $\mathbf{A_1}$–$\mathbf{A_4}$ were synthesized from 4-bromonaphthalic anhydride shown in Scheme 1 (With $\mathbf{A_4}$ as an example). Compounds $\mathbf{B_1}$–$\mathbf{B_4}$ were synthesized from 1,4,5,8-naphthalic anhydride in Scheme 2 (with $\mathbf{B_4}$ as an example). All of their structures were confirmed by $^1$H NMR, HRMS, and IR.

The structures of novel compounds are shown in Figure 2. It is found from Table 1 that compounds $\mathbf{A_1}$–$\mathbf{A_4}$, $\mathbf{B_1}$–$\mathbf{B_4}$ have very weak fluorescence and their maximal absorption wavelengths $\mathbf{A_1}$–$\mathbf{A_4}$, $\mathbf{B_1}$–$\mathbf{B_4}$ are about 347 and 377 nm, respectively, which quite matches with the DAPI excitation wavelengths of fluorescence microscopy (359 nm) and fluorescence scan ascent (345 nm).

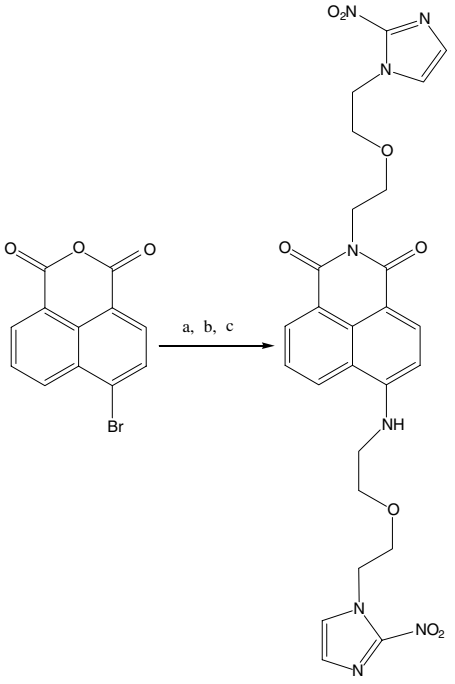


**Scheme 1.** Syntheses of target compounds $\mathbf{A_1}$–$\mathbf{A_4}$. Reagents and conditions: (a) 2-(2-aminoethoxy)ethanol, l-methyl-2-pyrrolidone, 110 °C, 2 h, 98% yield; (b) $Br_2/PCl_3$, ethyl acetate, reflux, 5 h, 82% yield; (c) 2-nitroimidazole or 3-nitro-l,2,4-triazole, $CH_3ONa$/DMF, reflux, 8 h, 52% yield.

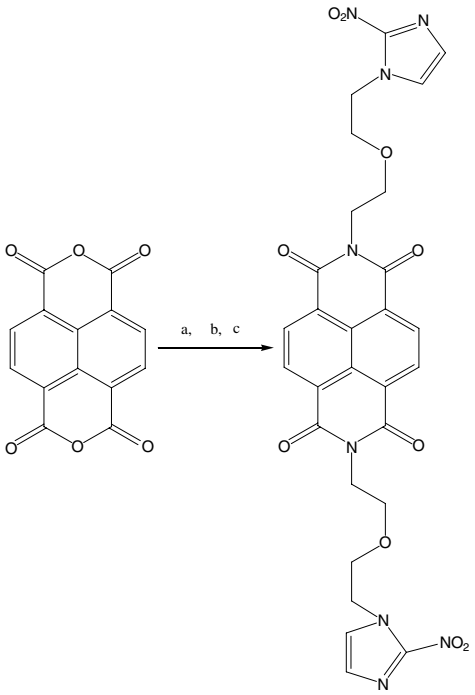


**Scheme 2.** Syntheses of target compounds $\mathbf{B_1}$–$\mathbf{B_4}$. Reagents and conditions: (a) 2-(2-aminoethoxy)ethanol, l-methyl-2-pyrrolidone, 100 °C, 2 h, 98% yield; (b) $Br_2/PCl_3$, ethyl acetate, reflux, 8 h, 80% yield; (c) 2-nitroimidazole or 3-nitro-l,2,4-triazole, $CH_3ONa$/DMF, reflux, 10 h, 48% yield.

**Table 1.** UV–vis and fluorescent data of $\mathbf{A_1}$–$\mathbf{A_4}$, $\mathbf{B_1}$–$\mathbf{B_4}$[a,b]

| Compound | UV $\lambda_{max}$/nm (lg $\varepsilon$) | FL $\lambda_{max}$/nm ($\Phi$) |
|---|---|---|
| $\mathbf{A_1}$ | 347 (4.05) | 450.5 (<0.0003) |
| $\mathbf{A_2}$ | 347 (4.02) | 455.5 (<0.0003) |
| $\mathbf{A_3}$ | 341 (4.18) | 391.0 (<0.0003) |
| $\mathbf{A_4}$ | 341 (4.19) | 394.0 (<0.0003) |
| $\mathbf{B_1}$ | 376 (4.30), 357 (4.26) | 404.7 (<0.0003) |
| $\mathbf{B_2}$ | 377 (4.32), 357 (4.27) | 404.5 (<0.0003) |
| $\mathbf{B_3}$ | 377 (4.31), 357 (4.25) | 402.0 (<0.0003) |
| $\mathbf{B_4}$ | 377 (4.37), 357 (4.35) | 403.5 (<0.0003) |

[a] In absolute methanol.
[b] With quinine sulfate in sulfuric acid as quantum yield standard ($\Phi$ = 0.55).

## 2.2. The time course of accumulation of fluorescent metabolites in CHO cells incubated with $\mathbf{A_4}$

Samples from hypoxic and oxic cell suspensions incubated with markers for various times were initially evaluated by fluorescence microscopy using appropriate excitation wavelengths. Further quantitative evaluation by fluorescence scan ascent was then carried out on promising compounds.

It has been reported that most hypoxic markers work well at the concentration of $10^{-4}$ M in different kind of cells.[3,9,10] In order to make sure whether this concentration of marker is best under our experimental conditions, we studied the time course of accumulation of fluorescent metabolites in CHO cells incubated with different concentrations of $\mathbf{A_4}$. The results are shown in Figure 3.

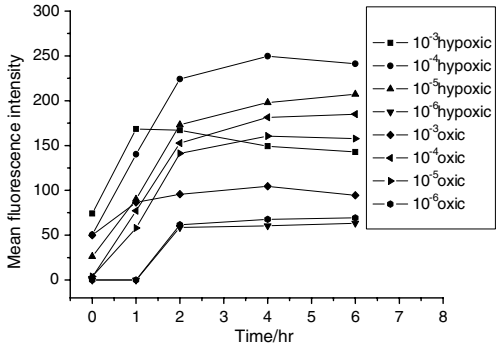


**Figure 3.** Typical time course of accumulation of fluorescent metabolites in CHO cells incubated with different concentrations of $\mathbf{A_4}$ at 37 °C by using fluorescence microscopy. The quantitative analysis on the fluorescent intensity was carried out by the fluorescent microscopy software furnished by Leica Co. Lit.

Figure 3 shows that when the concentration of compound ($\mathbf{A_4}$) was at $10^{-4}$ M and time was approaching to 2 h, the largest differential could be seen between the mean fluorescence intensities of cells incubated under hypoxic and oxic conditions. When the concentration of compound was at $10^{-3}$ M, the differential could be seen, but it was not as obvious as the one at $10^{-4}$ M. While when the concentration decreased to $10^{-5}$ M, the differential became smaller; as the concentration was $10^{-6}$ M, the differential became unapparent at all. One could easily see that $10^{-4}$ M was an appropriate concentration for our experiments, thus in the following work, all the compounds were incubated in cells under oxic and hypoxic conditions at $10^{-4}$ M.

## 2.3. The time course of development of fluorescence products in human highly metastatic lung carcinoma 95D cells with $\mathbf{A_4}$

The time course of development of fluorescence products in 95D cells with $\mathbf{A_4}$ under hypoxic and oxic conditions is shown in Figure 4. It showed that the fluorescence of cells incubated under hypoxic and oxic conditions, respectively, increased at the same speed during 2 h, thereby in the first stage, the hypoxic–oxic differential was very small. When time was approached

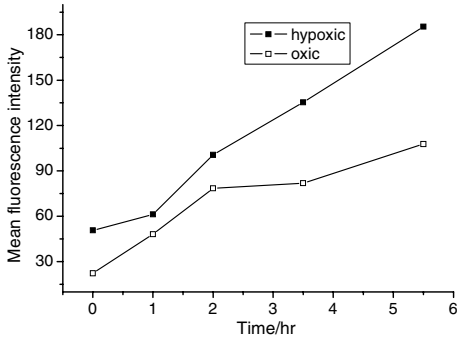


**Figure 4.** The time course of accumulation of fluorescent metabolites in 95D cells incubated with $10^{-4}$ M of $\mathbf{A_4}$ at 37 °C by using fluorescence microscopy. The quantitative analysis on the fluorescent intensity was carried out by the fluorescent microscopy software furnished by Leica Co. Lit.

to 2 h, with the further reduction of the compound in hypoxic cells, the fluorescence of cells went on to increase until time was approaching 5.5 h. While at the same time, the fluorescence of cells incubated under oxic condition kept at the same level. When the culture medium was under hypoxic condition for 6 h, most of the hypoxic cells would have been dead, thus the observation was ended. So, the largest hypoxic–oxic differential was found at 5.5 h.

### 2.4. The time course of development of fluorescence products in V79 379A Chinese hamster cells with $A_2$ and $A_4$

Figure 5 was the time courses of development of fluorescence products in V79 379A Chinese hamster cells with $\mathbf{A_2}$ and $\mathbf{A_4}$ under hypoxic and oxic conditions observed by fluorescence microscopy. Large differential can be seen between the fluorescence of cells. It is found that the fluorescence of cells incubated under oxic condition had little change all the time, but under hypoxic condition, it increased quickly during 3 h. The compounds $\mathbf{A_2}$ and $\mathbf{A_4}$ (with 2-nitroimidazole as reductive moiety) in hypoxic cells were reduced by nitroreductase enzymes in two-electron steps in an oxygen-insensitive process,[11] which resulted in significant increase of the fluorescence. When time was approaching 4 h, the reduction of compounds in hypoxic cells reached the maximal value and then kept it, of course, the hypoxic–oxic differential reached the largest at the same time.

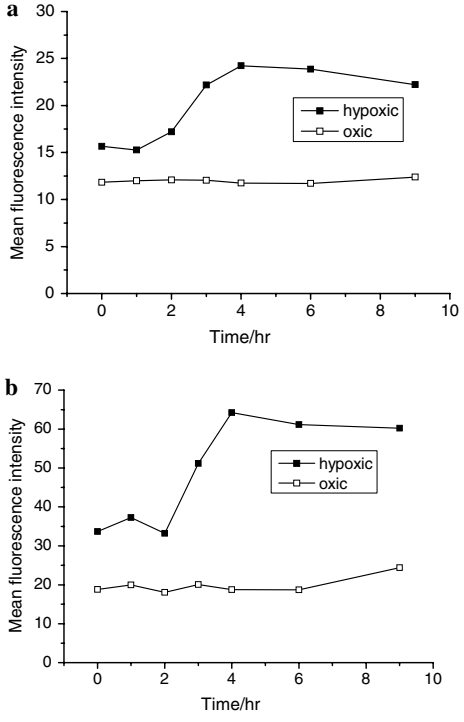


**Figure 5.** The time courses of accumulation of fluorescent metabolites in V79 cells incubated with $10^{-4}$ M of compounds at 37 °C by using fluorescence microscopy. (a) $\mathbf{A_2}$; (b) $\mathbf{A_4}$. The quantitative analysis on the fluorescent intensity was carried out by the fluorescent microscopy software furnished by Leica Co. Lit.

The fluorescence microphotographs of V79 cells incubated with $10^{-4}$ M of $\mathbf{A_2}$ and $\mathbf{A_4}$ are shown in Figures 6 and 7, respectively.

For the two promising compounds ($\mathbf{A_2}$ and $\mathbf{A_4}$) as hypoxic markers, further evaluation was carried out by fluo-

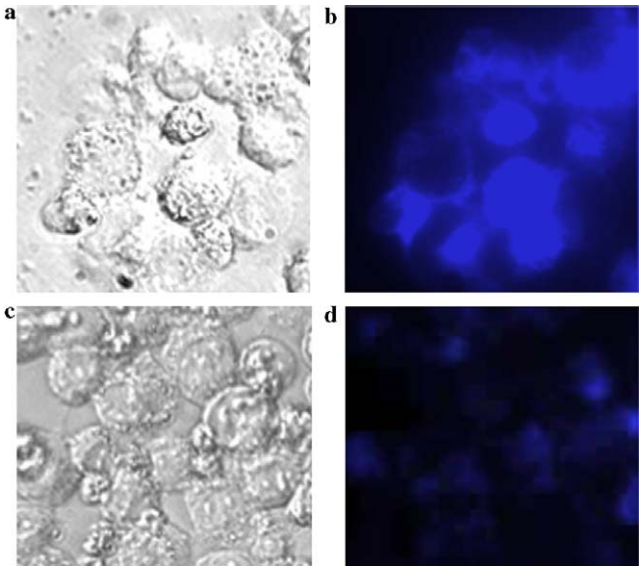


**Figure 6.** Fluorescence microphotographs of V79 cells incubated with $10^{-4}$ M of $\mathbf{A_2}$ at 37 °C. After 3.5 h incubation, scanning was taken. Magnification was 1000×. (a) Scanning was taken on brightfield, cells on hypoxic condition (incubated in nitrogen and 5% $CO_2$); (b) excited at 359 nm, cells on hypoxic condition; (c) scanning was taken on brightfield, cells on oxic condition (incubated in air and 5% $CO_2$); (d) excited at 359 nm, cells on oxic condition.

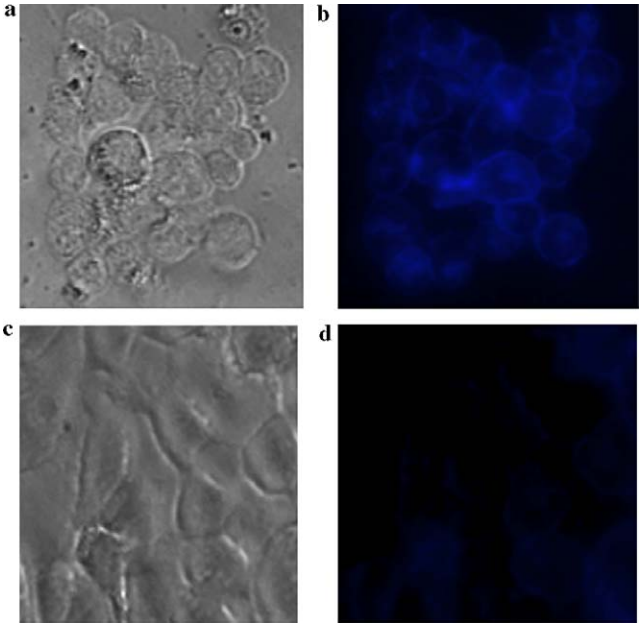


**Figure 7.** Fluorescence microphotographs of V79 cells incubated with 10–4 M of A4 at 37 °C. After 3.5 h incubation, scanning was taken. Magnification was 1000×. (a) Scanning was taken on brightfield, cells on hypoxic condition (incubated in nitrogen and 5% $CO_2$); (b) excited at 359 nm, cells on hypoxic condition; (c) scanning was taken on brightfield, cells on oxic condition (incubated in air and 5% $CO_2$); (d) excited at 359 nm, cells on oxic condition.

rescence scan ascent as shown in Figure 8. It was found that the largest hypoxic–oxic fluorescence differential of $\mathbf{A_4}$ in cells (20 times) was higher than $\mathbf{A_2}$ incubated in cells (15 times). The difference might have been caused by two reasons. On the one hand, the water solubility of $\mathbf{A_4}$ was improved when an ether moiety was introduced into the side chains as a hydrophilic group, which promoted the transport of compound in vivo to tumor cells. On the other hand, the fluorescence quenching by intramolecular photoinduced electron transfer (PET) from the reduction products of the nitroimidazole moiety to the napthalimide nucleus[8] of $\mathbf{A_4}$ was weaker than that of $\mathbf{A_2}$. After bioreduction the electron-deficient moiety of 2-nitroimidazole will become electron-rich moiety of 2-aminoimidazole, which is more easy to proceed PET to quench fluorescence somewhat, and balance the fluorescence enhancement during bioreduction. Because the side-chain length of $\mathbf{A_2}$ was shorter than that of $\mathbf{A_4}$, PET efficiency of the reduction product of $\mathbf{A_2}$ being higher than that of $\mathbf{A_4}$, and fluorescence quenching efficiency of $\mathbf{A_2}$'s reductive product also should be higher than that of $\mathbf{A_4}$, so that hypoxic–oxic fluorescence differential of $\mathbf{A_2}$ was lower than that of $\mathbf{A_4}$.

The study of the time courses of accumulation of fluorescent metabolites in CHO cells, 95D cells, and V79 cells incubated with $\mathbf{A_1}$ and $\mathbf{A_3}$ was also carried out with fluorescence scan ascent, the hypoxic–oxic fluorescence differential incubated with $\mathbf{A_1}$ and $\mathbf{A_3}$ in V79 cells being 3 times and 6 times, respectively. The difference between $\mathbf{A_1}$ and $\mathbf{A_3}$ was caused by the same two reasons as the case of $\mathbf{A_2}$ and $\mathbf{A_4}$.

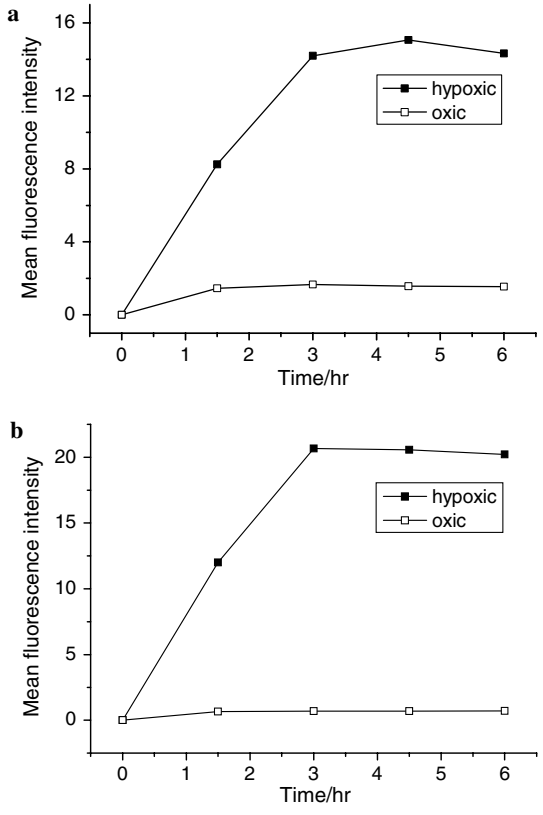


**Figure 8.** The time courses of accumulation of fluorescent metabolites in V79 cells incubated with $10^4$ M of compounds at 37 °C by using fluorescence scan ascent. (a) $\mathbf{A_2}$; (b) $\mathbf{A_4}$. The quantitative analysis on the fluorescent intensity was carried out by the fluorescence scan ascent of Leica Co. Lit.

The reason for the difference in fluorescence behavior between the two kinds of compounds $\mathbf{A_2}$, $\mathbf{A_4}$ and $\mathbf{A_1}$, $\mathbf{A_3}$ might have been that the electron-deficiency of 2-nitroimidazole was stronger than that of 3-nitro-l,2,4-triazole,[12] the electron-donating ability of the latter for bioreductive product was higher than that of the former. Therefore, the strong PET abilities to quench fluorescence for the reduction products of $\mathbf{A_1}$ and $\mathbf{A_3}$ by comparison with that of $\mathbf{A_2}$ and $\mathbf{A_4}$ balanced the fluorescence enhancement during bioreduction, which finally resulted in the little hypoxic–oxic fluorescence differential in cells for $\mathbf{A_1}$ and $\mathbf{A_3}$.

When compounds were incubated in CHO and 95D cells, the fluorescent intensity of cells on both hypoxic condition and oxic condition was strong (as shown in Figures 3 and 4), compounds having very limited selectivity for hypoxic cells and oxic cells. However, when compounds were in incubated in V79 cells, the fluorescent intensity of cells on oxic condition remained weak all the time, the one on hypoxic condition increased until reaching the maximal value, thus great differential fluorescence between hypoxic and oxic cells could be seen in V79 cells (Fig. 6).

When $\mathbf{B_1}$–$\mathbf{B_4}$ were incubated in CHO cells, 95D cells and V79 cells, only $\mathbf{B_4}$ in V79 cells showed 2.5 times hypoxic–oxic fluorescence differential, which resulted from a weak fluorescence of the reductive compound of **B**.

## 3. Conclusion

In summary, the present work demonstrated the design and evaluation of novel fluorescent markers for hypoxic cells. Two heterocyclic side chains were introduced into naphthalimide moiety in the fluorescent markers for a hypoxic cell study for the first time. Some of the compounds ($\mathbf{A_2}$ and $\mathbf{A_4}$) showed high differential fluorescence between hypoxic and oxic cells (V79 cells) in vitro, $\mathbf{A_4}$ also showing promising results in CHO cells and 95D cells in vitro. It verified that $\mathbf{A_2}$ and $\mathbf{A_4}$ could be promising candidate markers for hypoxic cells and were suitable for further evaluation as probes for hypoxic cells in tumors in vivo. The fluorescence microphotographs of cells were also obtained by fluorescence microscopy.

## 4. Experimental

### 4.1. Materials

All the solvents were of analytic grade. $^1$H NMR was measured on a Bruker AV-500 spectrometer with chemical shifts reported as parts per million (in acetone-$d_6$/DMSO-$d_6$/$CDCl_3$, TMS as an internal standard). Mass

spectra were measured on a HP 1100 LC–MS spectrometer. Melting points were determined with an X-6 micro-melting point apparatus and are uncorrected. Absorption spectra were determined on a PGENERAL TU-1901 UV–vis Spectrophotometer.

### 4.2. Synthesis

**4.2.1. General ($A_4$).** 4-Bromo-l,8-naphthalic anhydride reacted with 2-(2-aminoethoxy)ethanol at 110 °C for 2 h in 1-methyl-2-pyrrolidone. The cooled reaction mixture was poured into water and the yellow solid was collected by filtration. Then the crude product was dropped into ethyl acetate at 0 °C, after stirring for half hour, bromine and $PC1_3$ were added dropwise, and after refluxing for 5 h, the reaction liquid was concentrated and neutralized. When the pH value reached 5, the solid product was collected by filtration and crystallized from methanol/ethanol (6:1, v/v) to provide 2-[2-(2-bromo-ethoxy)-ethyl]-6-[2-(2-bromo-ethoxy)-ethylamino]-benzo[*de*]isoquinoline-1,3-dione. Sodium methoxide in methanol was added dropwise to a solution of 2-nitro-imidazole in DMF. After stirring for half hour, the solution was heated to 140 °C to boil off the methanol and then a solution of 2-[2-(2-bromo-ethoxy)-ethyl]-6-[2-(2-bromo-ethoxy)-ethylamino]-benzo[*de*]isoquinoline-l,3-dione in DMF was added and the mixture was heated at 150 °C for a further 8 h. The cooled reaction mixture was then poured into crushed ice and the crude product collected by filtration.

**4.2.2. 2-[2-(3-Nitro-[l,2,4]triazol-4-yl)-ethyl]-6-[2-(3-nitro-[l,2,4]triazol-4-yl)-ethylamino]-benzo[*de*]isoquinoline-1,3-dione ($A_1$).** The solid was separated with silica gel column chromatography using an eluent of ethyl acetate/petroleum ether (1:4, v/v). Mp >300 °C. $^1$H NMR (SF: 500 MHz, $CDCl_3$-$d_1$ $\delta$ (ppm): 8.70 (t, 2H, $J_1$ = 6.12 Hz, $J_2$ = 6.42 Hz), 8.46 (d, 1H, $J$ = 7.77 Hz), 8.13 (d, 1H, $J$ = 7.88 Hz), 7.94 (t, 1H, $J_1$ = 7.52 Hz, $J_2$ = 8.32 Hz), 7.27 (s, 2H, triazole-5′H), 4.91 (t, 2H, $J_1$ = 5.16 Hz, $J_2$ = 5.70 Hz, CON$CH_2$CH$_2$), 4.33 (t, 2H, $J_1$ = 6.32 Hz, $J_2$ = 6.25 Hz, NH$CH_2$CH$_2$), 3.92–3.90 (m, 2H, CON$CH_2$CH$_2$), 3.86–3.83 (m, 2H, NH$CH_2$CH$_2$). HRMS $C_{20}H_{16}N_{10}O_6$ calcd: 492.1254; found: 492.1258. IR (KBr): 3300, 3070, 2950, 1680, 1550 cm$^{-1}$.

**4.2.3. 2-[2-(2-Nitro-imidazol-l-yl)-ethyl]-6-[2-(2-nitro-imidazol-l-yl)-ethylamino]-benzo[*de*]isoquinoline-l,3-dione ($A_2$).** The solid was separated with silica gel column chromatography using an eluent of ethyl acetate/petroleum ether (2:5, v/v). Mp >300 °C. $^1$H NMR (SF: 500 MHz, acetone-$d_6$) $\delta$ (ppm): 8.20 (d, 1H, $J$ = 8.09 Hz), 8.11 (d, 1H, $J$ = 7.01 Hz), 7.85 (d, 1H, $J$ = 7.02 Hz, imidazole-5′H), 7.83 (d, 1H, $J$ = 7.03 Hz, imidazole-5′H), 7.78 (t, 1H, $J_1$ = 0.76 Hz, $J_2$ = 0.78 Hz), 7.65 (d, 1H, $J$ = 7.45 Hz), 7.56 (dd, 1H, $J_1$ = 7.10 Hz, $J_2$ = 7.10 Hz), 7.31 (d, 2H, $J$ = 7.07 Hz imidazole-4′H), 4.22 (t, 2H, $J_1$ = 6.47 Hz, $J_2$ = 6.43 Hz, CON$CH_2$CH$_2$), 4.17 (t, 2H, $J_1$ = 6.32 Hz, $J_2$ = 6.25 Hz, NH$CH_2$CH$_2$), 3.78 (t, 2H, $J_1$ = 6.21 Hz, $J_2$ = 6.27, CON$CH_2$C$_2$), 3.65 (t, 2H, NH$CH_2$C$_2$). HRMS $C_{22}H_{18}N_8O_6$ calcd: 490.1349, found: 490.1352. IR (KBr): 3300, 3070, 2950, 1680, 1550 cm$^{-1}$.

**4.2.4. 2-{2-[2-(3-Nitro-[l,2,4]triazol-4-yl)-ethoxy]-ethyl}-6-{2-[2-(3-nitro-[l,2,4]triazol-4-yl)-ethoxy]-ethylamino}-benzo[*de*]isoquinoline-l,3-dione ($A_3$).** The solid was separated with silica gel column chromatography using an eluent of ethyl acetate/petroleum ether (1:3, v/v). Mp >300 °C. $^1$H NMR (SF: 500 MHz, $CDCl_3$-$d_1$ $\delta$ (ppm): 8.69 (d, 1H, $J$ = 7.16 Hz), 8.61 (d, 1H, $J$ = 8.37 Hz), 8.44 (d, 1H, $J$ = 7.77 Hz), 8.07 (d, 1H, $J$ = 7.77 Hz), 7.88 (t, 1H, $J_1$ = 7.75 Hz, $J_2$ = 7.85 Hz), 7.26 (s, 2H, triazole-5′H), 4.62 (4H, t, $J_1$ = 6.93 Hz, $J_2$ = 6.93 Hz, 2$CH_2$CH$_2$OCH$_2$CH$_2$), 4.08 (t, 4H, $J_1$ = 6.04 Hz, $J_2$ = 6.14 Hz, 2CH$_2$CH$_2$OCH$_2$$CH_2$), 3.85 (t, 4H, $J_1$ = 6.56 Hz, $J_2$ = 6.58, 2CH$_2$$CH_2$OCH$_2$CH$_2$), 3.68 (t, 4H, $J_1$ = 6.96 Hz, $J_2$ = 6.95 Hz, 2CH$_2$CH$_2$O$CH_2$CH$_2$). HRMS $C_{24}H_{24}N_{10}O_8$ calcd: 580.1778; found: 580.1775. IR (KBr): 3320, 1680, 1550 cm$^{-1}$.

**4.2.5. 2-{2-[2-(2-Nitro-imidazol-l-yl)-ethoxy]-ethyl}-6-{2-[2-(2-nitro-imidazol-l-yl)-ethoxy]-ethylamino}-benzo[*de*]isoquinoline-l,3-dione ($A_4$).** The solid was separated with silica gel column chromatography using an eluent of ethyl acetate/petroleum ether (1:2, v/v). Mp > 300 °C. $^1$H NMR (SF: 500 MHz, acetone-$d_6$) $\delta$ (ppm): 8.04 (d, 1H, $J$ = 7.16 Hz), 7.99 (d, 1H, $J$ = 7.97 Hz), 7.69 (d, 1H, $J$ = 7.52 Hz, imidazole-5′H), 7.67 (d, 1H, $J$ = 7.69 Hz, imidazole-5′H),7.65 (dd, 1H, $J_1$ = 5.55 Hz, $J_2$ = 5.90 Hz), 7.46–7.41 (m, 2H), 7.123 (d, 1H, $J$ = 6.0), 7.121 (d, 1H, $J$ = 4.63), 4.22 (t, 4H, $J$ = 5.29, $J_2$ = 6.04, 2$CH_2$CH$_2$OCH$_2$CH$_2$), 3.94 (t, 4H, $J_1$ = 7.06, $J_2$ = 7.12, 2CH$_2$$CH_2$OCH$_2$CH$_2$), 3.93 (t, 4H, $J_1$ = 7.12, $J_2$ = 7.10, 2CH$_2$CH$_2$OCH$_2$CH$_2$), 3.53 (t, 2H, $J_1$ = 4.55 Hz, $J_2$ = 5.15 Hz, CH$_2$CH$_2$O$CH_2$CH$_2$), 3.52 (t, 2H, $J_1$ = 4.69 Hz, $J_2$ = 4.38 Hz, CH$_2$CH$_2$O$CH_2$CH$_2$). HRMS $C_{26}H_{26}N_8O_8$ calcd: 578.1873; found: 578.1875. IR (KBr): 3320, 1680, 1550 cm$^{-1}$.

**4.2.6. 2,7-Bis-[2-(3-nitro-[l,2,4]triazol-l-yl)-ethyl]-benzo-[*lmn*][3,8]phenanthroline-l,3,6,8-tetraone ($B_1$).** The solid was separated with silica gel column chromatography using an eluent of ethyl acetate/petroleum ether (1:5, v/v). Mp >300 °C. $^1$H NMR (SF: 500 MHz, DMSO-$d_6$), $\delta$ (ppm), 8.64 (s, 4H, naphtha), 7.24 (s, 2H, triazole-5′H), 4.16 (t, 4H, $J_1$ = 6.44 Hz, $J_2$ = 6.35 Hz, 2-$NCH_2$CH$_2$–),3.64 (t, 4H, $J_1$ = 6.32 Hz, $J_2$ = 6.47 Hz, 2-NCH$_2$CH$_2$–); HRMS $C_{22}H_{16}N_{10}O_8$ calcd: 548.1153; found: 548.1152. IR (KBr): 3100, 2850, 1680, 1550 cm$^{-1}$.

**4.2.7. 2,7-Bis-[2-(2-nitro-imidazol-l-yl)-ethyl]-benzo[*lmn*]-[3,8]phenanthroline-l,3,6,8-tetraone ($B_2$).** The solid was separated with silica gel column chromatography using an eluent of ethyl acetate/petroleum ether (1:4, v/v). Mp >300 °C. $^1$H NMR (SF: 500 MHz, DMSO-$d_6$), $\delta$ (ppm), 8.49 (s, 4H, naphtha), 8.42 (d, 2H, $J$ = 8.97, imidazole-5′H), 7.06 (d, 2H, $J$ = 8.45, imidazole-4′H), 3.99 (t, 4H, $J_1$ = 6.43 Hz, $J_2$ = 6.36 Hz, 2-N$CH_2$CH$_2$–), 3.48 (t, 4H, $J_1$ = 6.36 Hz, $J_2$ = 6.38 Hz, 2-NCH$_2$$CH_2$–); HRMS $C_{24}H_{18}N_8O_8$ calcd: 546.1248; found: 546.1250. IR (KBr): 3100, 2850, 1680, 1550 cm$^{-1}$.

**4.2.8. 2,7-Bis-{2-[2-(3-nitro-[l,2,4]triazol-l-yl)-ethoxy]-ethyl}-benzo[*lmn*][3,8]phenanthroline-l,3,6,8-tetraone ($B_3$).** The solid was separated with silica gel column chroma-

tography using an eluent of ethyl acetate/petroleum ether (1:3, v/v). Mp >300 °C. $^1$H NMR (SF: 500 MHz, DMSO-$d_6$), $\delta$ (ppm), 8.75 (s, 4H, naphtha), 7.06 (s, 2H, triazole-5′H), 4.33 (t, 4H, $J_1 = 6.19$ Hz, $J_2 = 6.18$ Hz, 2-N$CH_2$CH$_2$O–), 3.85 (t, 2H, $J_1 = 6.23$, $J_2 = 6.32$, $CH_2$OCH$_2$, 3.84 (t, 2H, $J_1 = 6.32$, $J_2 = 6.33$, $CH_2$OCH$_2$), 3.45–3.43 (m, 4H), 3.33 (t, 4H, $J_1 = 5.39$, $J_2 = 5.36$, 2-OCH$_2$$CH_2$–); HRMS $C_{26}H_{24}N_{10}O_{10}$ calcd: 636.1677; found: 636.1675. IR (KBr): 3100, 2850, 1680, 1550 cm$^{-1}$.

**4.2.9. 2,7-Bis-{2-[2-(2-nitro-imidazol-l-yl)-ethoxy]-ethyl}-benzo[*lmn*] [3,8]phenanthroline-l,3,6,8-tetraone ($B_4$).** The solid was separated with silica gel column chromatography using an eluent of ethyl acetate/petroleum ether (1:3, v/v). Mp >300 °C. $^1$H NMR (SF: 500 MHz, DMSO-$d_6$), $\delta$(ppm), 8.68 (s, 4H, naphtha), 7.86 (d, 2H, $J = 5.96$, imidazole-5′H), 7.26 (d, 2H, $J = 8.13$, imidazole-4′H), 4.25 (t, 4H, $J_1 = 6.19$ Hz, $J_2 = 6.18$ Hz, 2-N$CH_2$CH$_2$O–), 4.05 (t, 4H, $J_1 = 4.58$ Hz, $J_2 = 4.60$ Hz, 2-NCH$_2$CH$_2$O), 3.69 (t, 4H, $J_1 = 6.16$ Hz, $J_2 = 5.89$ Hz, 2-$CH_2$CH$_2$), 3.63 (t, 4H, $J_1 = 4.66$ Hz, $J_2 = 4.53$ Hz, 2-OCH$_2$$CH_2$–); HRMS $C_{28}H_{26}N_8O_{10}$ calcd: 634.1772; found: 634.1775. IR (KBr): 3100, 2850, 1680, 1550 cm$^{-1}$.

### 4.3. Biology

Because of the poor water solubility for some compounds used in this work, many of the compounds were initially dissolved at $(1–2) \times 10^{-2}$ M in dimethylsulfoxide (DMSO), and small volumes were added to cell suspensions to give the appropriate marker concentration. The final concentration of DMSO was 1% (v/v) or less. Then the suspension was incubated in special gases (air + 5% $CO_2$, nitrogen + 5% $CO_2$) at 37 °C. Then samples from hypoxic and oxic cell suspensions incubated with markers for various times were evaluated by fluorescence microscopy. Further evaluation by fluorescence scan ascent was then carried out on promising compounds for their higher sensitivity.

CHO cells were maintained in Eagle's minimal essential medium with Earle's salts, modified for suspension culture with 10% fetal calf serum. 95D cells were maintained in Eagle's minimal essential medium with Earle's salts, modified for suspension culture, with 15% fetal calf serum. V79 379A Chinese hamster cells were maintained as exponentially growing suspension cultures in Eagle's minimal essential medium with Earle's salts, modified for suspension culture with 7.5% fetal calf serum.

The quantitative analyses on fluorescent intensity in Figures 3–5 were carried out by the fluorescent microscopy software furnished by Leica Co. Lit. (DMIR 6800). The analysis in Figure 8 was carried out by fluorescence scan ascent of Leica Co. Lit.

## Acknowledgments

The National Basic Research Program of China (2003CB114400), the National Key Technologies R&D Program (Grant 2005BA711A04), National Natural Science Foundation of China, The Science and Technology Foundation of Shanghai, and The Education Commission of Shanghai partially supported this study.

## References and notes

1. Raleigh, J. A. *Semin. Radiat. Oncol.* **1996**, *6*, 1.
2. (a) Fyles, A. W.; Miolsevic, M.; Wong, R.; Kavanagh, M. C.; Pintilie, M.; Sun, A.; Chapman, W.; Levin, W.; Manchul, L.; Keane, T. J.; Hill, R. P. *Radiother. Oncol.* **1998**, *48*, 149; (b) Al-Hallaq, H. A.; River, J. N.; Zamora, M.; Oikawa, H.; Karczmar, G. S. *Int. Radiat. Oncol. Biol. Phys.* **1998**, *41*, 151; (c) Karen, A. Y.; Siham, B. P.; Rachelle, M. L.; Darrell, Q. B.; Matthew, C. F.; James, S. B.; Gerald, E. H.; Chapman, J. D. *Int. Radiat. Oncol. Biol. Phys.* **1995**, *33*, 111.
3. Wardman, P.; Clarke, E. D.; Hodgkiss, R. J. *Int. J. Radiat. Oncol. Biol. Phys.* **1984**, *10*, 1344.
4. (a) Mason, R. P.; Holtzman, J. L. *Biochem. Biophys. Res. Commun.* **1975**, *67*, 1267; (b) Wardman, P.; Clarke, E. D. *Biochem. Biophys. Res. Commun.* **1976**, *69*, 942.
5. Heimbrook, D. C.; Sartorelli, A. C. *Mol. Pharmacol.* **1986**, *29*, 168.
6. (a) Varghese, A. J.; Whitmore, G. F. *Cancer Res.* **1980**, *40*, 2165; (b) Varghese, A. J.; Whitmore, G. F. *Cancer Res.* **1983**, *43*, 78.
7. (a) Franko, A. J.; Koch, C. J.; Garrecht, B. M.; Sharplin, J.; Hughes, D. *Cancer Res.* **1987**, *47*, 5367; (b) HOdgkiss, R. J.; Jones, G.; Long, A.; Parrick, J.; Smith, K. A.; Stratford, M. R. L.; Wilson, G. D. *Br. J. Cancer* **1991**, *63*, 119.
8. Begg, A. C.; Hodgkiss, R. J.; McNally, N. J.; Middleton, R. W.; Stratford, M. R. L.; Terry, N. H. A. *Br. J. Radiol.* **1985**, *58*, 645.
9. (a) Stratford, M. R. L.; Clarke, E. D.; Hodgkiss, R. J.; Middleton, R. W.; Wardman, P. *Int. J. Radiat. Oncol. Biol. Phys.* **1984**, *10*, 1353; (b) Hodgkiss, R. J.; Begg, A. C.; Middleton, R. W.; Parrick, J.; Stratford, M. R. L.; Wardman, P.; Wilson, G. D. *Biochem. Pharmacol.* **1991**, *41*, 533; (c) Hodgkiss, R. J.; Middleton, R. W.; Parrick, J.; Rami, H. K.; Wardman, P.; Wilson, G. D. *J. Med. Chem.* **1992**, *35*, 1920; (d) Hodgkiss, R. J.; Parrick, J.; Manuchehr, P.; Stratford, M. R. L. *J. Med. Chem.* **1994**, *37*, 4352.
10. Hodgkiss, R. J.; Jones, G. W.; Anthony, L.; Middleton, R. W.; Parrick, J.; Stratford, M. R. L.; Wardman, P.; Wilson, D. *J. Med. Chem.* **1991**, *34*, 2268.
11. Hodgkiss, R. J. *Anti-Cancer Drug Des.* **1998**, *13*, 687.
12. Baggott, J. E.; Pilling, M. J. *J. Chem. Soc., Faraday Trans. 1* **1983**, *79*, 221.